



## Distribution and generation characteristics of halogenated acetic acids disinfection by-products in reclaimed water

Juncheng Wang, Jina Song\*

*College of Energy and Environmental Engineering, Hebei University of Engineering, Handan City, Hebei Province, 056038, China, Tel.: +86 17303101318; email: songjina@126.com (J. Song), Tel.: +86 15650145176; email: wjc2077@foxmail.com (J. Wang)*

Received 19 January 2023; Accepted 15 April 2023

---

### ABSTRACT

In this study, the secondary effluent organic matter (EfOM) was divided into hydrophobic acid (HOA), hydrophobic base, hydrophobic neutral (HON), and hydrophilic components by using the wastewater from a sewage treatment plant as reclaimed water. The correlation between the type and structure of each component and the possible by-products of halogenated acetic acids (HAAs) produced within 30 min and 5 d after chlorination was investigated. The number of disinfection by-products and conventional water quality indicators were assessed. The results showed that the main HAAs species formed at 30 min were dominated by bromochloroacetic acid, dichloroacetic acid (DCAA), and monobromoacetic acid (accounting for 93.05% of the total generation). However, the main HAA species formed at 5 d were trichloroacetic acid, bromodichloroacetic acid, and DCAA (accounting for 88.76% of the total generation). HON in EfOM has a molecular weight of 5–10 kDa. Soluble microbial products (SMPs) carrying hydroxyl groups, amine groups, and benzene rings are the primary source of HAAs, accounting for 61.56% of the 30-min generation amount and 37.52% of the 5-day yield. Following HOA component, the molecular weight is similar to HON component, containing unsaturated carboxyl COO<sup>-</sup>, SMPs of aromatic hydrocarbons, humic acid, and fulvic acid organic compounds. The theoretical results of exploring the existence and related characteristics of disinfection by-products in EfOM can offer practical advice.

*Keywords:* Effluent organic matter; Component separation; Disinfection by-products; Molecular weight; Fluorescence spectroscopy

---

### 1. Introduction

At the same time as the shortage of drinking water, industrial and agricultural water consumption continues to increase, the shortage of available water resources is severe, and finding unconventional water sources becomes a priority [1]. After advanced biological treatment, the secondary effluent is further treated as reclaimed water, alleviating water shortage. Reclaimed water's safety and harmlessness are among the most important concerns for people [2].

The secondary effluent contains many toxic and hazardous substances that biological methods cannot remove, such as dissolved organic matter (DOM), antibiotics, heavy

metals, etc. [3]. Chlorination of reclaimed water is an effective and experienced disinfection method; however, the reactions between secondary effluent organic matter (EfOM) and chlorine produces many disinfection by-products (DBPs). Studies [4] have shown that DBPs are cytotoxic, extremely difficult to remove, and may cause various human diseases, including genotoxicity, asthma, skin rashes, and colon cancer [5]. Besides, DBPs will harm the growth, development and reproduction of aquatic organisms and destroy the balance of aquatic ecosystems [6]. EfOM is a disinfection by-product formation precursor (DBPFP) that needs to be removed whenever possible [7]. Research shows halogenated acetic acids (HAAs) account for about 14% of

---

\* Corresponding author.

chlorinated disinfection by-products (DBPs) [8]. HAAs include monochloroacetic acid (MCAA), dichloroacetic acid (DCAA), trichloroacetic acid (TCAA), monobromoacetic acid (MBAA), dibromoacetic acid (DBAA), tribromoacetic acid (TBAA), bromochloroacetic acid (BCAA), bromodichloroacetic acid (BDCAA), chlorodibromoacetic acid (CDBAA) [9].

A few researchers have concentrated on the predictive parameters for producing HAAs. Beauchamp's et al. [10] research found that  $UV_{254}$  can correlate the optimal amount of coagulant with the removal rate of DBPFP. Li et al. [11] used three water sources as subjects and found that the characterization of DBPFP showed that DBPs were not associated with dissolved organic carbon (DOC) values. Furthermore, Ramavandi et al. [12] came to the same conclusion. However, knowing the indicative parameters of HAAs does not provide complete control over their generation. Therefore, more researchers began to investigate the hydrophilicity of HAAs precursors. Although the most organic matter is hydrophobic acid (HOA) component, Zhao et al. [13] found that hydrophobic neutral (HON) component is the most important precursor to HAAs, due to hydrophobic substances carrying more electrons and having a larger molecular weight. Hong et al. [1] found that hydrophobic acids and the rest of the non-transphilic organic matter (hydrophobic organic matter that does not convert to hydrophilic substances) are the main precursors to TCAA. Nevertheless, Wang's et al. [14] study discovered that hydrophilic (HI) component are more likely to produce HAAs. Currently, most research is focused on the HAAs generation characteristics of surface water and drinking water sources. Because the deep excavation of organic structures is less likely to cause by-product formation, more research on effluent organic matter is required.

Due to the biological treatment process has a significant impact on EfOM, it was divided into four components: hydrophobic acid (HOA), hydrophobic base (HOB), HON, and hydrophilic (HI), and its ability to produce HAAs was carefully examined. The composition distribution and structural properties of EfOM by-product formation after chlorination were investigated for secondary treatment reuse in sewage plants. Determination of unsaturated aromatic degree, content, and proportion of each component of organic matter by DOC and  $UV_{254}$ , the molecular weight (MW) was determined by liquid chromatography size exclusion chromatography (LC SEC), the three-dimensional excitation-emission matrix (3D-EEM) and synchronous fluorescence spectroscopy (SFS) were determined to determine the type of organic matter in EfOM; scanning ultraviolet absorption spectroscopy (UV-Vis) and Fourier-transform infrared spectroscopy (FTIR) to explore the functional groups carried by each component in effluent organic matter; Gas chromatography (GC) was used to determine the amount and potential of HAAs formation after chlorination for 30 min and 5-days, and to study the correlation between the physicochemical properties of each component of effluent organic matter and the formation of HAAs, and to provide theoretical support for the selection of relevant water treatment materials and technologies for subsequent advanced treatment. The water plant can selectively optimize the treatment process of the secondary effluent, reduce the difficulty of the subsequent treatment process and improve the treatment efficiency.

## 2. Experimental method and analysis

### 2.1. Component separation

Before separating EfOM, the resin was activated with methanol and cleaned with pure water [15]. When the effluent is neutral after elution, proceed as follows: (1) The chromatography column was filled with XAD-8 resin to a height of about 10 cm, and the water sample was raised to a height of about 30 cm to bring down the outflow liquid, and 500 mL of water was sampled and filtered through a 0.45  $\mu\text{m}$  cellulose acetate membrane. Wash the resin column with 500 mL of 0.1 mol/L HCl solution. HOB component is present in the effluent, and the resin adsorbs the HON component. (2) After the effluent passing through the resin column is adjusted to pH2 with concentrated HCl, the effluent is the HI component, and the resin adsorbs the HOA component simultaneously. (3) The effluent is HOA component after eluting the resin column with 0.1 mol/L NaOH. (4) For 24 h, a Soxhlet extraction was performed on a resin column using methanol. Methanol dissolved in HON component was then placed in a beaker, fully volatilized at 50°C and dissolved in 500 mL of pure water to produce the HON component. After completion of all steps, the four component solutions are adjusted to pH7 and stored for future use.

### 2.2. By-product extraction

The water sample was taken from the secondary effluent of a three-tank oxidation ditch process of a sewage treatment plant. After the water sample passed through a 0.45  $\mu\text{m}$  filter membrane, it was stored at 25°C in the dark. As a chlorine oxidant, sodium hypochlorite was utilized, with a density of 1.17 g/cm<sup>3</sup> and an effective rate of roughly 10%. To decide precisely the amount of chlorine added, after separating organic matter from 200 mL of water in a brown glass bottle, add 10, 20, 40, 60, 80, and 100  $\mu\text{L}$  of sodium hypochlorite solution, and measure the 5-day generation of HAAs. The results showed that when the dosage was 80  $\mu\text{L}$ , the HAAs all showed a flat trend. The generation amounts almost no longer increased, so the optimal dosage of 30 min and 5-day generation potential was determined to be 80  $\mu\text{L}$ .

Put 200 mL of the water sample to be measured in a brown glass bottle, add 80  $\mu\text{L}$  of sodium hypochlorite solution, and keep it at 25°C in the dark for 5 d before adding 1 mL of sodium thiosulfate to stop the reactions. After the reaction, place 40 mL of the water sample in the separating funnel, then add 2 mL of sulfuric acid, 8 g of sodium chloride to shake and dissolve until there are no white particles, 6 mL of MTBE, extract for 3 min, and stand for 3 min, then collect the lower aqueous phase. Pipette 3.0 mL of extract into a 15 mL colorimetric tube, add 30 mL of internal standard solution, then 3 mL of the freshly made sulfuric acid-methanol solution to mix well, derive it in a hot water bath at 50°C for 120 min, remove the colorimetric tube, cool to room temperature, add 7 mL of sodium chloride solution, tighten the cap and shake well, and then use a 10 mL graduated pipette to remove the lower portion of the sample. Pipette 1.0 mL of the upper extract into a brown injection bottle with a capacity of 2 mL and wait for injection determination.

The test repeats the sample preparation steps and draws the HAAs standard by the experimental data curve.

To prepare the sample, place six parts of 40 mL pure water in a separatory funnel. Add 0, 10, 20, 50, 100, and 200  $\mu\text{L}$  of the HAAs mixed standard solution, respectively. Only seven HAAs were investigated in the experiment since the experimental study discovered that two HAAs (CDBAA and TBAA) are also formed in pure water. The detection limit is 2  $\mu\text{g/L}$ , and the recovery percentage of substitutes spiked in the sample range is 91.2%–108%.

### 2.3. Instrument parameters

A gas chromatograph was used to identify and quantify HAAs (HP 6890N Agilent, USA). The column was a quartz capillary column of 30 m length, 0.32 mm inner diameter, 0.25  $\mu\text{m}$  film thickness, and a 5% phenyl/95% dimethylpolysiloxane stationary phase. The inlet temperature is 210°C. The heating procedure is as follows: start at 40°C for 5 min, then gradually increase to 65°C at 2.5°C/min, then 85°C at 10°C/min, and finally 205°C for 1 min. The detector has a temperature of 300°C. The carrier gas is nitrogen; the carrier gas flow rate was 2.0 mL/min, and the tail-blowing air flow rate was 60 mL/min. The injection volume is 2.0  $\mu\text{L}$  and is non-split.

A total organic carbon analyzer produced by Shimadzu (Japan) was used to analyze TOC. The TU-1901 UV-Vis spectrophotometer determined UV-Vis and  $\text{UV}_{254}$ . EEM and SFS were analyzed and measured by a fluorescence spectrometer (Hitachi F7100, Japan). The relative molecular weight was determined by a liquid chromatograph (Shimadzu LC-2030, Japan), the chromatographic column was Zenix SEC-100, and the UV detector was used with wavelengths of 220 and 254 nm.

EfOM and its four separate components are placed at 55°C to dry to powder to obtain samples. The samples were prepared by the potassium bromide grinding method [16], Fourier measured the FTIR transform infrared spectrometer (Shimadzu IRA affinity, Japan), the data were analyzed by OMNIC software (second derivative Norris), and the number of smoothing points was 11.

## 3. Results and discussion

### 3.1. Conventional water quality indicators

Fig. 1 showed that the relationship between the DOC contents of each component was  $\text{HOA} > \text{HI} > \text{HON} > \text{HOB}$ , and

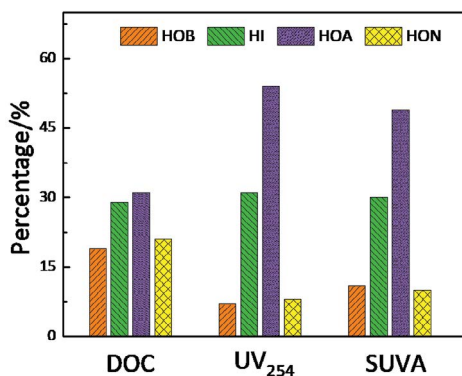


Fig. 1. Percentage of dissolved organic carbon,  $\text{UV}_{254}$ , SUVA for each component in effluent organic matter.

the proportion of each component was 31%, 29%, 21%, and 19%, respectively. There was an apparent gradient relationship between the components. The hydrophobic substances accounted for 71%, and the hydrophilic substances accounted for 29%. Wang et al. [1] also came to a similar conclusion that EfOM and natural organic matter (NOM) in natural rivers have a certain degree of similarity in the characteristics of hydrophilicity and hydrophobicity.

The  $\text{UV}_{254}$  value usually represents the humic acid content in the water sample. The proportion of each component of EfOM is consistent with the DOC value; the  $\text{UV}_{254}$  values of effluent organic matter are  $\text{HOA} (54\%) > \text{HI} (31\%) > \text{HON} (8\%) > \text{HOB} (7\%)$ . The hydrophobic material accounts for 73%, and the hydrophilic material accounts for 31%; The  $\text{UV}_{254}$  value of HOA component is the largest, which preliminarily shows that HOA component contains low-polymerized unsaturated fatty acids, carbon-carbon double bonds, aromatic carboxylic acids, and phenolic substances, and contains more aromatic hydrocarbon organic substances [17], followed by HI, HON, and HOB components.

Under certain conditions,  $\text{SUVA} = \text{UV}_{254}/\text{DOC}$  [specific UV absorbance (SUVA)] can initially represent the unsaturated aromaticity among EfOM and the potential for DBPs generation [18]; Aromaticity represents the saturation degree of organic matter. It is an important indicator of whether it is easy to produce DBPs by substitution reaction and addition reaction with chlorine and bromine ions. The proportion of SUVA of EfOM components preliminarily indicates that HOA component (49%) has the highest unsaturated aromaticity. This feature implies that HOA component contributes the most to the production of DBPs, which are susceptible to chlorination, to produce disinfection by-products, followed by HI (30%), HOB (11%), and HON components (10%).

Fig. 2 shows that HOA and HI components have distinct characteristic peaks at 215 and 220 nm, respectively, and that HI component has a slightly higher absorbance, indicating that HI component contains more chromophores (e.g., carbonyls, nitro, etc.) than HOA component; HOB component has absorption peaks of benzene rings or heterocyclic aromatic hydrocarbons around 200 nm [18]; HON component has almost no absorption peak above 200 nm, indicating that HON component is a saturated compound, such as cycloalkane, saturated carboxylic acid, carboxyl ester, and other substances with isolated carbon-carbon double bonds [19].

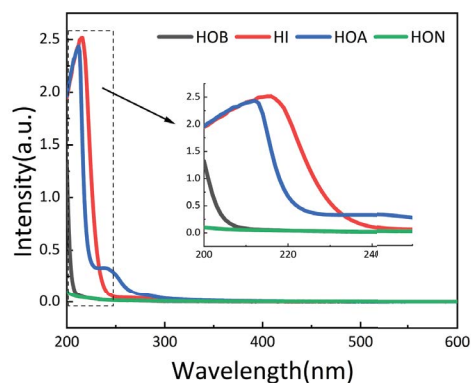


Fig. 2. UV-Vis of four components in effluent organic matter.

### 3.2. Excitation-emission matrix

FRI uses the different fluorescence intensities of excitation wavelength and the emission wavelength to determine the type of organic matter and divides EfOM into five regions corresponding to several types of substances [20], which are tyrosine protein, tryptophan protein, and fulvic acid substances (FA), soluble microbial products (SMPs), and humic acids (HA), the EEMs of the four components in EfOM are shown in Fig. 3. Ma's et al. [21] studies also showed that the hydrophilic part comprises FA, SMPs, and HA.

The typical fluorescent peak of the SMPs A is visible in the EEM images of different raw water constituents. The characteristic response peak of SMPs in the HON component spectrum is the most visible since most of the bacteria in the bio pool can survive in a neutral condition, and the pH level is generally steady. In addition to SMPs in each component, HI component also has HA and FA characteristic peaks, HON component appears to have a response peak of complex proteins and benzene cyclin-containing substances, and HOA component has HA characteristic peaks; it is worth noting that HOB component only contains SMPs. The characteristic peaks of HA, FA, and SMPs in HOA and HI components are rich in various unsaturated groups, such as aromatic benzene rings, conjugated double bonds, and carboxyl groups [22].

The DOC values corresponding to the various components of EfOM are similar, but the degrees of fluorescence in the EEM image are differ. Among them, the characteristic fluorescence peaks of HON are more apparent, and the characteristic peaks of HOB, HI, and HOA components are

not prominent. The fluorescence intensity of EfOM depends on the functional groups of the molecule [23]. Electron-donor functional groups, such as the amine and hydroxyl groups, can increase the fluorescence intensity of the DOM. In contrast, electron-acceptor-type functional groups, such as the carboxyl group, can reduce the fluorescence intensity of the DOM [22]. Therefore, it is speculated that HON is rich in amine and hydroxyl groups, and HOB, HI, and HOA components are rich in carboxyl groups.

### 3.3. Synchronous fluorescence spectrum

The excitation and emission wavelength of SFS has always maintained a fixed wavelength distance. This particular measurement method can reduce the overlap of spectra and weaken the influence of light scattering, thereby simplifying the spectrum and making it easier to analyze the measured spectrum [24]; The synchronous fluorescence setting measured wavelength difference  $\Delta\lambda = 50$  nm, ( $\Delta\lambda = \lambda_{EM} - \lambda_{EX}$ ), and the excitation wavelength was 200–550 nm; The slit width of the excitation unit is 5 nm, and the negative high voltage of the photocell is 400 V. According to the position of characteristic peaks in SFS, it can be divided into three types of substances [25], as shown in Table 1.

Fig. 4 shows the characteristic peak response degrees of each component of EfOM in different regions; HOB, HI, and HOA components all have response peaks of protein-like fluorescent substances and fulvic acid-like fluorescent substances in regions I and II. According to the different response peaks, the contents of the three are as

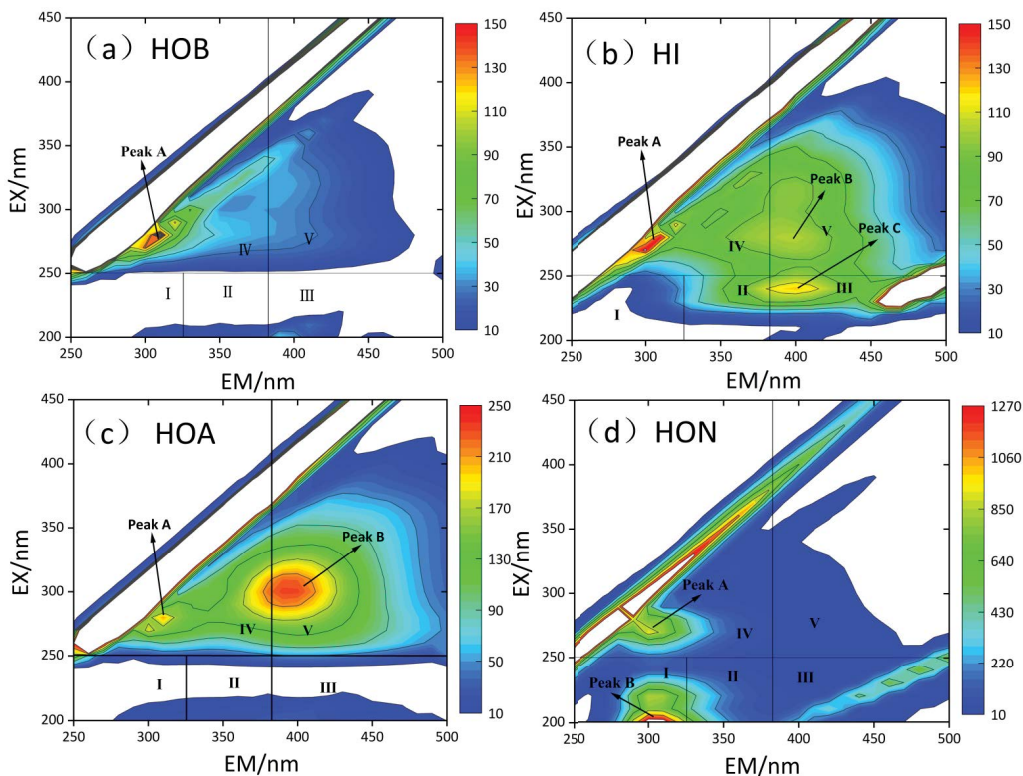


Fig. 3. Excitation-emission matrix for each component in effluent organic matter.

follows: HON, HOB, HI, and HOA components. In particular, the HON component has a strong absorption peak in region I, indicating that it contains a lot of protein-like fluorescent substances.

### 3.4. Molecular weight

Fig. 5a shows that the characteristic [26] peaks of each component of EfOM representing carboxyl and aromatic

Table 1

Substances corresponding to different regions of the fluorescence spectrum

Project	Wavelength (nm)	Corresponding substances
I	250–300	Protein-like fluorescent substance
II	300–380	Fulvic acid-like fluorescent substance
III	380–550	Humic acid-like fluorescent substance

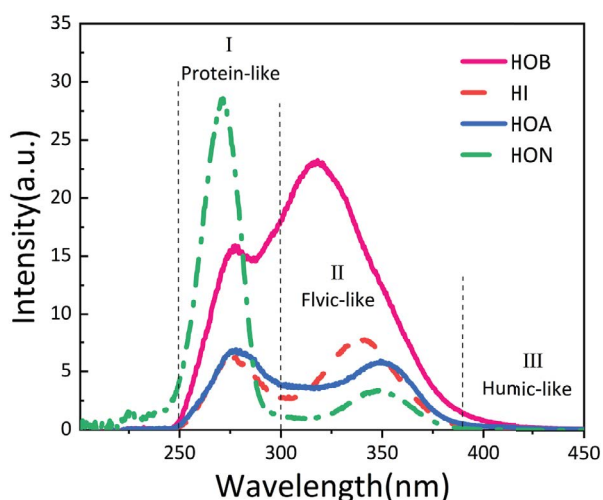


Fig. 4. Synchronous fluorescence spectroscopy of the four components in effluent organic matter.

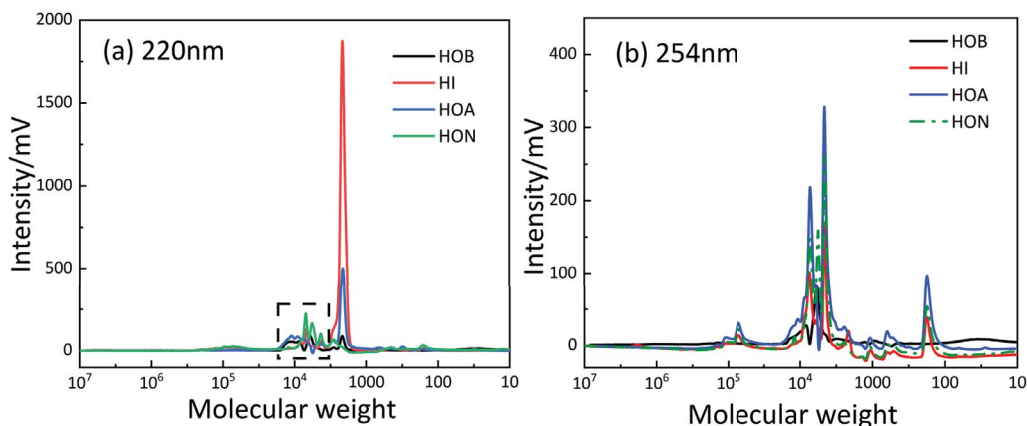


Fig. 5. Molecular weight distribution at 220 and 254 nm of effluent organic matter components.

chromophores appear between 1 and 10 kDa at the UV absorption wavelength of 220 nm. The peak of HI is the highest at 3 kDa, indicating that the molecular weight of HI components is mostly 3 kDa, followed by HOA; HON and HOB components have weak characteristic peaks at 8 kDa. According to Fig. 5b, it can be seen that EfOM represents the characteristic peak of aromatic group organic matter at 254 nm, mainly located between 1 and 10 kDa, and the characteristic peak intensity, in turn, is HOA, HON, HI, and HOB components; The first three have certain similarities, the molecular weight is mainly 5–10 kDa medium molecular substances, followed by 100–500 Da small molecule substances, containing a small amount of 5–10 kDa macromolecular substances; HOB component are mainly medium molecular substances.

The absorbance at 254 nm is a standard method for calculating HA content [27], and HA is a crucial component of DOC [28]. Furthermore, 220 nm absorbance is related to carboxylic acids and aromatic groups susceptible to substitution reactions to form chlorination by-products, which is related to the substance's ability to generate DBPs [27].

### 3.5. Fourier-transform infrared spectroscopy

After drying at 55°C, the components of EfOM showed different shapes. HI component showed a white crystalline structure, HOB component turned into an orange powder, and HOA component appeared as a brown-red powder. After dehydration with the same amount of water, the content of each component decreased, followed by HI, HOA, HOB, and HON components. Because HON component needs to be dissolved in methanol first, it is challenging to extract. Although HON component that are extremely difficult to extract are not obtained for FTIR testing, it can be judged from the abnormally high fluorescence peaks of HON component that SMPs and proteins of HON component carry a large number of chromophores such as carboxylic acids, which are prone to substitution reactions and generate disinfection by-products. Moreover, HON component only has more fulvic acid substances than HOB component, so the relevant characteristics can be obtained by referring to the HOB component analogy. HON component is a substance that needs special attention in reclaimed water treatment.

Fig. 6 shows that each component in EfOM exhibits O–H and N–H vibrations around 3,700–3,800  $\text{cm}^{-1}$  [16]; HI component exhibits –COOH stretching vibration at 3,400  $\text{cm}^{-1}$ , COO-symmetric carboxyl group [20] appeared around 1,390  $\text{cm}^{-1}$ , and the other components did not appear; HOB, HI and HON components both have a characteristic peak of slight vibration of benzene ring around 1,500–1,600  $\text{cm}^{-1}$ , C–H stretching vibration of saturated carbon appears at 2,970  $\text{cm}^{-1}$ , and the O=C=O group appears near 2,300–2,400  $\text{cm}^{-1}$  vibration and the benzene ring vibration at 1,630  $\text{cm}^{-1}$ .

The HOB component exhibits asymmetric vibrations of –COOH and C–O contained in alcohols, esters, and phenols at 1,140–1,160  $\text{cm}^{-1}$ , and chlorination increases the

content of C–O groups [29]; The HOB and HI components appeared C=C characteristic peaks around 1,640  $\text{cm}^{-1}$ , and the HOA component showed weak absorption peaks. It was further confirmed that the unsaturation of the HOA component mainly came from unsaturated aromatic hydrocarbons or carboxyl groups rather than the C=C structure. Only the HOA component exists as the vibration of the benzene ring substituent C–H at 600–870  $\text{cm}^{-1}$  [30]. It is worth noting that the C–H group is prone to substitution reaction with chlorine to produce chlorinated disinfection by-products. One of the best measures of an organic compound’s capacity to generate DBPs is the number of functional groups it carries that are susceptible to substitution and addition reactions.

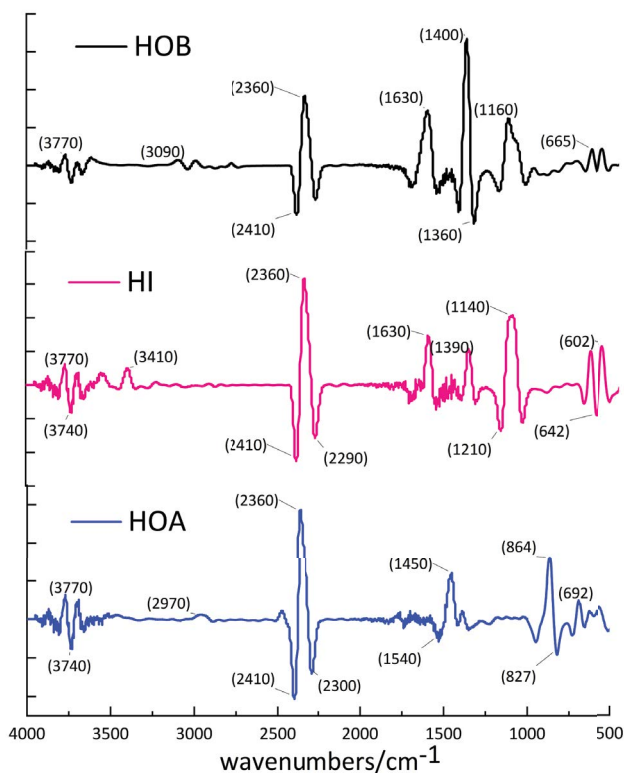


Fig. 6. Fourier-transform infrared spectroscopy second derivative plot of hydrophobic base, hydrophilic, and hydrophobic acid components in effluent organic matter.

### 3.6. Generation potential and amount of HAAs

Figs. 7a and 8a show that TCAA, BDCAA, and MCAA are the most generated HAAs after various chlorinating components of EfOM for 30 min, accounting for 93.05% of the total HAAs generated. The contribution of HON component DBPs is the highest, accounting for 61.56%, followed by HOA: 14.78%, HI: 11.84%, and HOB: 11.82%; The DOC and SUVA of the HOA component were 12% and 38% higher than those of the HON component, respectively, but the number of by-products produced by HON was much higher than that of the HOA component. This result is very different from the possibility of the formation of HAAs of each component shown by DOC and SUVA. Li et al. [11] research also shows DOC is not associated with DBPs generation potentials. It is worth noting that HOB component only produces BCAA, DCAA, and MBAA, of which BCAA produces much more than the other two; the total generation of MCAA, TCAA, BDCAA, and DBAA is less than 5  $\mu\text{g/L}$ , which is negligible; SMPs and complex proteins dominated HON component, and benzene rings carry a variety of substitutable groups, which are easy to chlorinate with chlorine and produce DBPs. Bromine and iodide ions hardly participate in the chlorination reaction of EfOM after chlorination for 30 min, so many HAAs are not detected [31]. Although  $\text{UV}_{254}$  cannot directly represent the ability of organic matter to produce HAAs, Beauchamp’s et al. [32] research shows that the value of  $\text{UV}_{254}$  has no apparent correlation with the potential of DBPs generation. However, there is a specific correlation between  $\text{UV}_{254}$  and coagulant dosage, which is hardly affected by season.

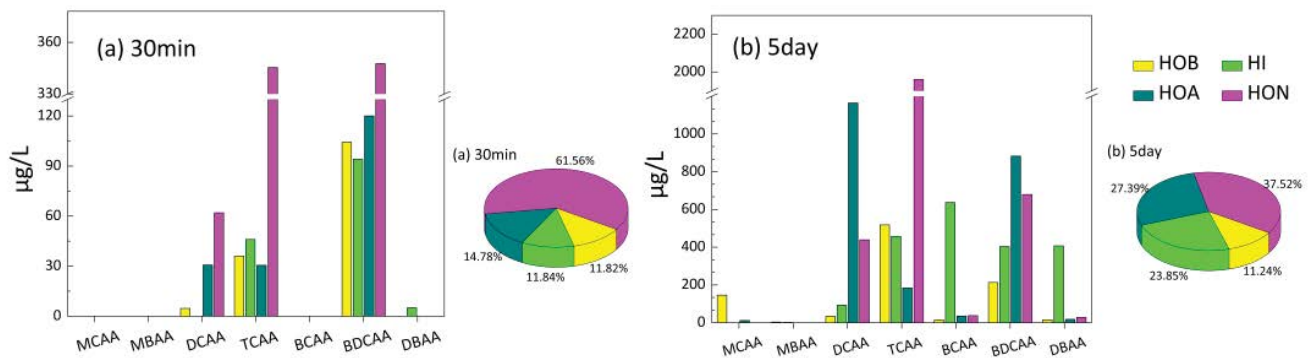


Fig. 7. Effluent organic matter components correspond to 30 min (a) and 5 d (b) halogenated acetic acids generation.

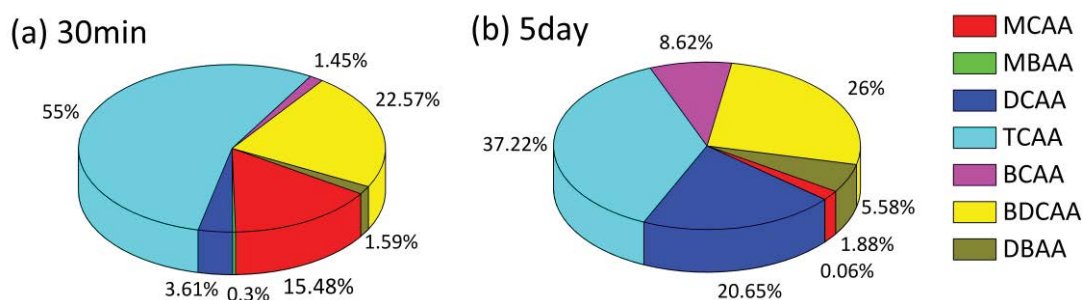


Fig. 8. Percentage of each component of effluent organic matter and the percentage of halogenated acetic acids.

Figs. 7b and 8b show that the formation potential of each component of EfOM corresponds to HAAs: HON component mainly generates TCAA, BDCAA, and DCAA; HOA component mainly generates DCAA, BDCAA, and TCAA; HI mainly generates BCAA, TCAA, and DBAA; HOB component mainly generates TCAA, BDCAA, and MCAA; It is worth noting that the generation potential of HOB component to generate MCAA accounted for 93% of each component, and the detection amount of other components was negligible. The amount of MBAA produced did not change significantly due to the long reaction time after chlorination. The aromatic content in the large organic molecules in the HON component can react with chlorine to form aromatic nonhalogenated DBPs, and then form aromatic halogenated DBPs. At the same time, the intermediate product DBP can be decomposed into aliphatic halogenated DBP in the presence of chlorine [33]. The specific performance is shown in Fig. 7; the generation of TCAA, BDCAA and DCAA increased significantly when the chlorination time was 5 d.

The seven HAAs are in the following order: TCAA > B DCAA > DCAA > BCAA > DBAA > MCAA > MBAA, and the first three accounted for 88.76% of the total generation. Although the total amount of HON component organic matter is small, according to EEM and SFS, the HON component contains many fluorescent chromophore proteins and SMPs, so it is easy to undergo substitution and addition reactions with chlorine to produce HAAs. This result shows high consistency with Hong et al. [1] and Zhao et al. [13]. The HON component fraction that produces HAAs had the highest 5-day generation potential, accounting for 37.52% of the total generation potential, followed by HOA: 27.39%, HI: 23.85%, and HOB: 11.24%. It shows the same characteristics as the formation potential of HAAs after chlorination of each component for 30 min. As an indicator of DBPs' generation potential, DOC and SUVA are too dependent on water quality. When SMPs dominate DOC in water samples, the SUVA value is generally low because its cellular structure does not contain unsaturated aromatic hydrocarbons. The correlation between SUVA value and DBPs was extremely poor in this case ( $R^2 \leq 0.5$ ); when  $SUVA < 2$ , EEM fluorescence characteristics and component analysis should be used as auxiliary parameters [34].

The DOC of the HI component accounted for 29% of EfOM, and  $UV_{254}$  accounted for 31% of EfOM; the proportion of HAAs produced within 30 min and 5 d were only 11.84% and 23.85%, respectively. DOC values are correlated with the low content of DOM species in the raw water. However,

hydrophobic substances will generate some hydrophilic intermediate and final products during water treatment. Therefore, the content of HI component after advanced treatment may increase, and the corresponding HAAs produced by HI component will also increase [13]. According to the molecular weight results, it can be judged that the ability of each component to produce by-products is not directly related to the molecular weight. Nowadays, a portable EEM tester has been developed that can perform preliminary organic matter category exams on the site of a sewage plant, measure other parameters after the pretreatment of water samples, and formulate corresponding operation parameters of the water treatment process based on various data.

#### 4. Conclusions

- After separating the four components of EfOM, hydrophobic substances accounted for 71% of the total DOC and 73% of the total  $UV_{254}$ , and the content of hydrophobic substances was much higher than that of hydrophilic organic substances. The aromaticity degree represented by the SUVA value could not accurately indicate the amount and potential of HAAs. However, the combined analysis of the fluorescence characteristics of EEM and SUVA could more accurately predict the amount and potential of HAAs.
- The 30-min generation amount and 5-d formation potential from HAAs of hydrophobic organics are 85.22% and 72.61%, respectively, indicating that hydrophobic organics are the main precursors of by-products of HAAs; the main products of HAAs generation potential are BCAA, DCAA, and MBAA, which account for the total amount. 93.05%; the main products of HAAs 5-d formation potential are TCAA, BDCAA, and DCAA, which account for 88.76% of the total; SMPs of HON component, which accounts for a low proportion in EfOM, are the primary generation source; and a small amount of macromolecular HON component is in the process of chlorination reaction. It becomes many small molecular substances, followed by HOA component containing carboxyl groups and unsaturated aromatic hydrocarbons.
- HON component accounts for 61.56% and 37.52% of the total amount of HAAs 30-min generation and 5-d formation potential, respectively. Its molecular weight is mainly medium molecular weight substances of 5–10 kDa, followed by a bit small molecular weight substances of 100–500 Da, and large molecular weight organic matter

of 50–100 kDa, containing saturated states, SMPs containing amine groups, hydroxybenzene rings, fatty acids, and complex proteins; followed by HOA component containing COO<sup>-</sup>, O=C=O, benzene ring, and unsaturated aromatic hydrocarbons, which accounted for 15% and 27%, respectively, and whose molecular weight distribution is the same as HON component.

### Acknowledgments

The research was financially supported by the Program for Science and Technology Research of Universities in Hebei Province (ZD2021022), the National Natural Science Foundation of China (51908177) and the Natural Science Foundation of Hebei Province (E2021402015).

### References

- [1] H.C. Hong, F.Q. Huang, F.Y. Wang, L.X. Ding, H.J. Lin, Y. Liang, Properties of sediment NOM collected from a drinking water reservoir in South China, and its association with THMs and HAAs formation, *J. Hydrol.*, 476 (2013) 274–279.
- [2] W. Ahmed, M. Kitajima, S. Tandukar, E. Haramoto, Recycled water safety: current status of traditional and emerging viral indicators, *Curr. Opin. Environ. Sci. Health*, 16 (2020) 62–72.
- [3] L. Alexandrou, B.J. Meehan, O.A.H. Jones, Regulated and emerging disinfection by-products in recycled waters, *Sci. Total Environ.*, 637 (2018) 1607–1616.
- [4] H.C. Hong, Y.C. Lu, X.Y. Zhu, Q. Wu, L.G. Jin, Z.G. Jin, X.X. Wei, G.C. Ma, H.Y. Yu, Cytotoxicity of nitrogenous disinfection by-products: a combined experimental and computational study, *Sci. Total Environ.*, 856 (2023) 159273, doi: 10.1016/j.scitotenv.2022.159273.
- [5] X. Wei, M. Yang, Q. Zhu, E.D. Wagner, M.J. Plewa, Comparative quantitative toxicology and QSAR modeling of the haloacetonitriles: forcing agents of water disinfection by-product toxicity, *Environ. Sci. Technol.*, 54 (2020) 8909–8918.
- [6] M.T. Yang, X.R. Zhang, Comparative developmental toxicity of new aromatic halogenated DBPs in a chlorinated saline sewage effluent to the marine polychaete *Platynereis dumerilii*, *Environ. Sci. Technol.*, 47 (2013) 10868–10867.
- [7] J.L. Lin, A.R. Ika, Minimization of halogenated DBP precursors by enhanced PACl coagulation: the impact of organic molecule fraction changes on DBP precursors destabilization with Al hydrates, *Sci. Total Environ.*, 703 (2020) 134936, doi: 10.1016/j.scitotenv.2019.134936.
- [8] R.K. Padhi, S. Subramanian, K.K. Satpathy, Formation, distribution, and speciation of DBPs (THMs, HAAs, ClO<sup>2-</sup> and ClO<sup>3-</sup>) during treatment of different source water with chlorine and chlorine dioxide, *Chemosphere*, 218 (2019) 540–550.
- [9] R. Mompremier, Ó.A.F. Mariles, J.E.B. Bravo, K. Ghebremichael, Study of the variation of haloacetic acids in a simulated water distribution network, *Water Supply*, 19 (2019) 88–96.
- [10] N. Beauchamp, C. Bouchard, C. Dorea, M. Rodriguez, Ultraviolet absorbance monitoring for removal of DBP-precursor in waters with variable quality: enhanced coagulation revisited, *Sci. Total Environ.*, 717 (2020) 137225, doi: 10.1016/j.scitotenv.2020.137225.
- [11] A.Z. Li, X. Zhao, R. Mao, H.J. Liu, J.H. Qu, Characterization of dissolved organic matter from surface waters with low to high dissolved organic carbon and the related disinfection by-product formation potential, *J. Hazard. Mater.*, 271 (2014) 228–235.
- [12] B. Ramavandi, S. Farjadfar, M. Ardjmand, S. Dobaradaran, Effect of water quality and operational parameters on trihalomethane formation potential in Dez River water, Iran, *Water Resour. Ind.*, 11 (2015) 1–12.
- [13] Y.M. Zhao, F. Xiao, D.S. Wang, M.Q. Yan, Z. Bi, Disinfection by-product precursor removal by enhanced coagulation and their distribution in chemical fractions, *J. Environ. Sci.*, 25 (2013) 2207–2213.
- [14] D.S. Wang, Y.M. Zhao, M.Q. Yan, C.W.K. Chow, Removal of DBP precursors in micro-polluted source waters: a comparative study on the enhanced coagulation behavior, *Sep. Purif. Technol.*, 118 (2013) 271–278.
- [15] X.M. Sun, C.Y. Wu, Y.X. Zhou, W. Han, Using DOM fraction method to investigate the mechanism of catalytic ozonation for real wastewater, *Chem. Eng. J.*, 369 (2019) 100–108.
- [16] W. Chen, N. Habibul, X.Y. Liu, G.P. Sheng, H.Q. Yu, FTIR and synchronous fluorescence heterospectral two-dimensional correlation analyses on the binding characteristics of copper onto dissolved organic matter, *Environ. Sci. Technol.*, 49 (2015) 2052–2058.
- [17] P. Rakruam, S. Wattanachira, Reduction of DOM fractions and their trihalomethane formation potential in surface river water by in-line coagulation with ceramic membrane filtration, *J. Environ. Sci.*, 26 (2014) 529–536.
- [18] C.J. Williams, D. Conrad, D.N. Kothawala, H.M. Baulch, Selective removal of dissolved organic matter affects the production and speciation of disinfection by-products, *Sci. Total Environ.*, 652 (2019) 75–84.
- [19] M.A. Zazouli, S. Nasser, A.H. Mahvi, A.R. Mesdaghinia, M. Younejian, M. Gholami, Determination of hydrophobic and hydrophilic fractions of natural organic matter in raw water of Jalalieh and Tehranspars water treatment plants (Tehran), *J. Appl. Sci.*, 7 (2007) 2651–2655.
- [20] J.N. Song, X. Jin, X.C. Wang, P.K. Jin, Preferential binding properties of carboxyl and hydroxyl groups with aluminium salts for humic acid removal, *Chemosphere*, 234 (2019) 478–487.
- [21] D.F. Ma, B.Y. Gao, C.F. Xia, Y. Wang, Q.Y. Yue, Q. Li, Effects of sludge retention times on reactivity of effluent dissolved organic matter for trihalomethane formation in hybrid powdered activated carbon membrane bioreactors, *Bioresour. Technol.*, 166 (2014) 381–388.
- [22] Q. Han, H. Yan, F. Zhang, N. Xue, Y. Wang, Y.B. Chu, B.Y. Gao, Trihalomethanes (THMs) precursor fractions removal by coagulation and adsorption for bio-treated municipal wastewater: molecular weight, hydrophobicity/hydrophilicity and fluorescence, *J. Hazard. Mater.*, 297 (2015) 119–126.
- [23] B. Bruijns, R. Tiggelaar, H. Gardeniers, Dataset of the absorption, emission and excitation spectra and fluorescence intensity graphs of fluorescent cyanine dyes for the quantification of low amounts of dsDNA, *Data Brief*, 10 (2016) 132–143.
- [24] S.B. Marina, E. Saioa, C.B. Yannick, A.G. Ryder, Investigating native state fluorescence emission of Immunoglobulin G using polarized excitation-emission matrix (pEEM) spectroscopy and PARAFAC, *Chemom. Intell. Lab. Syst.*, 185 (2019) 1–11.
- [25] P.K. Jin, J.N. Song, X.C. Wang, X. Jin Two-dimensional correlation spectroscopic analysis on the interaction between humic acids and aluminum coagulant, *J. Environ. Sci.*, 64 (2018) 181–189.
- [26] L.C. Hua, S.J. Chao, C. Huang, Fluorescent and molecular weight dependence of THM and HAA formation from intracellular algal organic matter (IOM), *Water Res.*, 148 (2019) 231–238.
- [27] G. Korshin, C.W.K. Chow, R. Fabris, M. Drikas, Absorbance spectroscopy-based examination of effects of coagulation on the reactivity of fractions of natural organic matter with varying apparent molecular weights, *Water Res.*, 43 (2009) 1541–1548.
- [28] M.S. Siddique, X.J. Xiong, H.K. Yang, T. Maqbool, N. Graham, W.Z. Yu, Dynamic variations in DOM and DBPs formation potential during surface water treatment by ozonation-nanofiltration: using spectroscopic indices approach, *Chem. Eng. J.*, 427 (2022) 132010, doi: 10.1016/j.cej.2021.132010.
- [29] A. Sardana, B. Cottrell, D. Soulsby, T.N. Aziz, Dissolved organic matter processing and photoreactivity in a wastewater treatment constructed wetland, *Sci. Total Environ.*, 648 (2019) 923–934.
- [30] Z.P. Liu, W.H. Wu, P. Shi, J.S. Guo, J. Cheng, Characterization of dissolved organic matter in landfill leachate during the

- combined treatment process of air stripping, Fenton, SBR and coagulation, *Waste Manage.*, 41 (2015) 111–118.
- [31] Y.X. Sun, Q.Y. Wu, H.Y. Hu, J. Tian, Effects of operating conditions on THMs and HAAs formation during wastewater chlorination, *J. Hazard. Mater.*, 168 (2009) 1290–1295.
- [32] N. Beauchamp, C. Bouchard, C. Dorea, M. Rodriguez, Ultraviolet absorbance monitoring for removal of DBP-precursor in waters with variable quality: enhanced coagulation revisited, *Sci. Total Environ.*, 717 (2020) 137225, doi: 10.1016/j.scitotenv.2020.137225.
- [33] J.Y. Jiang, X.R. Zhang, X.H. Zhu, Y. Li, Removal of intermediate aromatic halogenated DBPs by activated carbon adsorption: a new approach to controlling halogenated DBPs in chlorinated drinking water, *Environ. Sci. Technol.*, 51 (2017) 3435–3444.
- [34] L.C. Hua, S.J. Chao, K. Huang, C. Huang, Characteristics of low and high SUVA precursors: relationships among molecular weight, fluorescence, and chemical composition with DBP formation, *Sci. Total Environ.*, 727 (2020) 138638, doi: 10.1016/j.scitotenv.2020.138638.